THIRD EUROPEAN ROTORCRAFT AND POWERED LIFT AIRCRAFT FORUM

PAPER n° 51

HELICOPTER REDUCTION GEAR : FREQUENCIES AND MODE SHAPES

M. LALANNE - P. TROMPETTE - J. DER HAGOPIAN

J. LAFON - M. CONTE

I.N.S.A. Laboratoire de Mécanique des Structures

20, avenue Albert Einstein 69621 Villeurbanne - France

September 7-9-1977

Aix en Provence - France

ASSOCIATION AERONAUTIQUE ET ASTRONAUTIQUE DE FRANCE

INTRODUCTION

In mechanics and more specifically in aeronautics light structures have to be designed in order to have the highest performances for the systems such as satellites, rockets, jets, helicopters. A consequence of this is that many frequencies of resonance are low and may be easily excited. It is then necessary to control the vibrations occuring in these structures. Generally vibration control can be performed by at least two ways. In the first a mathematical model of the structure is built and used to predict the frequencies and associated mode shapes. This model, now generally based on a finite element technique, allows a simple determination of the influence of modifications of the structure. In the second way, as in the first it is possible to change the values of the resonance frequencies but generally not to cancel them, some damping is added in the structure to have limited amplitudes at each resonance.

Here we present the problem of a reduction gear. It is an axisymetric rotating structure whose parts are thin or thick. Here only the equations of a thick rotating structure are presented and the finite element method is used. Displacements will be developped in Fourier's series and the Coriolis effect will be neglected [1], [2], [3], [4], [5], mode shapes have been obtained from holographic measurements and both finite elements and experimental results at rest are compared.

DIFFERENTIAL EQUATIONS OF THE STRUCTURE

The differential equations of the structure are obtained from the following steeps. Kinetic energy T and potential strain energy U are calculated, then the finite element method is used and at last Lagrange's equations are applied :

$$\frac{d}{dt}\left(\frac{\partial T}{\partial \delta^{\circ}}\right) - \frac{\partial T}{\partial \delta} + \frac{\partial U}{\partial \delta} = 0 \qquad (1)$$

with δ, nodal displacement vector.

The dot indicates derivative with respect to time.
$R1(r_1,\theta_1,z_1)$ is an absolute coordinate system and z_1 axis of symetry of the structure is also axis of rotation. $R_2(r_2,\theta_2,z_2)$ is an coordinate system fixed to the rotating structure, z_2 is the same axis as z_1.

The coordinates in R_2 of a typical point M of the structures are a, b, c. Due to the structure deformation the coordinates of M become $a + u_r$, $b + u_\theta$, $c + u_z$ and the velocity of M expressed by its components in R_2 is :

$$\vec{V}_M = \begin{bmatrix} u^{\circ}_r \\ u^{\circ}_\theta \\ u^{\circ}_z \end{bmatrix} + \begin{bmatrix} 0 \\ 0 \\ \Omega \end{bmatrix} \Lambda \begin{bmatrix} a + u_r \\ b + u_\theta \\ c + u_z \end{bmatrix} = \begin{bmatrix} u^{\circ}_r - \Omega(b + u_\theta) \\ u^{\circ}_\theta + \Omega(a + u_r) \\ u^{\circ}_z \end{bmatrix} \qquad (2)$$

with Ω, speed of rotation.

The kinetic energy is expressed by :

$$T = \frac{1}{2}\int_\tau \rho . V^t\ V\ d\tau \qquad (3)$$

with ρ, mass per unit volume
t, matrix transposition symbol

and may be written, using (2), as :

$$T_1 = T_1 + T_2$$

where

$$\begin{aligned} T_1 &= \frac{1}{2}\int_\tau \rho(u^{\circ}{}_r{}^2 + u^{\circ}{}_\theta{}^2 + u^{\circ}{}_z{}^2)d\tau + \frac{\Omega^2}{2}\int_\tau (u_r{}^2 + u_\theta{}^2)d\tau \\ &+ \Omega\int_\tau \rho(u_r u^{\circ}{}_\theta - u^{\circ}{}_r u_\theta)d\tau + \Omega^2\int_\tau \rho\ a\ u_r\ d\tau \qquad (4) \\ T_2 &= \Omega\int_\tau \rho\ a\ u^{\circ}{}_r\ d\tau + \frac{\Omega^2}{2}\int_\tau \rho(a^2+b^2)d\tau - \Omega^2\int_\tau \rho\ b\ u_\theta\ d\tau \\ &- \Omega\int_\tau \rho\ b\ u^{\circ}{}_r\ d\tau \end{aligned}$$

T_2 includes all the terms of T whose influence in the equations of the systems due to (1) and the expressions of the displacements functions is equal to zero.

The displacements functions will be choosen as :

$$\begin{aligned} u_r &= \sum_{n=0}^{N} u_{rn}(r,z)\ .\ \mathrm{Cos}\ n\theta \\ u_z &= \sum_{n=0}^{N} u_{zn}(r,z)\ .\ \mathrm{Cos}\ n\theta \qquad (5) \\ u &= \sum_{n=0}^{N} u_{\ n}(r,z)\ .\ \mathrm{Sin}\ n\theta \end{aligned}$$

with n, Fourier's series order.

Due to the orthogonality properties of the trigonometric functions in the interval $0 - 2\pi$, integrals of (4) are independant of angular position θ and only dependant of the cross section geometry of the structure and the Fourier's series order n.

Toroidal finite elements are used with triangular cross-section, 3 nodes and 3 displacements at each node.
Applying for the whole structure (1) :

$$\frac{d}{dt}\left(\frac{\partial T}{\partial \delta^{\circ}}\right) - \frac{\partial T}{\partial \delta} = \sum_{n=0}^{N} (M_n\ \delta^{\circ\circ}{}_n + C_n \delta^{\circ}{}_n - \Omega^2 M_{gn}\delta_n - \alpha_n . F(\Omega^2)) \qquad (6)$$

with :

$\alpha_n = 1$ for $n = 0$

$\alpha_n = 0$ for $n \neq 0$

δ_n, nodal displacement vector for n

M_n, classical mass matrix

C_n, Coriolis matrix

$\Omega^2 M_{gn}$, supplementary stiffness matrix

$F(\Omega^2)$, centrifugal force vector

The potential strain energy is obtained from :

$$U = \frac{1}{2} \int_\tau \sigma^t \cdot \varepsilon \, d\tau \tag{7}$$

with :

σ, stress vector
ε, strain vector

and

$$\sigma = D \cdot \varepsilon \tag{8}$$

Where D is the elasticity matrix function of the characteristics of the material : E, Young's modulus and ν, Poisson's ratio for isotropic systems.

From (7) and (8) :

$$U = \frac{1}{2} \int_\tau \varepsilon^t \, D \, \varepsilon \, d\tau \tag{9}$$

The second order expressions of the strain vector ε will be used to take into account the rotation effect. Their expressions are :

$$\begin{aligned}
\varepsilon_{rr} &= \frac{\partial u_r}{\partial r} + \frac{1}{2}\left[\left(\frac{\partial u_r}{\partial r}\right)^2 + \left(\frac{\partial u_z}{\partial r}\right)^2 + \left(\frac{\partial u_\theta}{\partial r}\right)^2\right] \\
\varepsilon_{zz} &= \frac{\partial u_z}{\partial z} + \frac{1}{2}\left[\left(\frac{\partial u_r}{\partial z}\right)^2 + \left(\frac{\partial u_z}{\partial z}\right)^2 + \left(\frac{\partial u_\theta}{\partial z}\right)^2\right] \\
\varepsilon_{\theta\theta} &= \frac{u_r}{r} + \frac{1}{r}\frac{\partial u_\theta}{\partial \theta} + \frac{1}{r^2}\left[\left(\frac{\partial u_r}{\partial \theta}\right)^2 + \left(\frac{\partial u_z}{\partial \theta}\right)^2 + \left(\frac{\partial u_\theta}{\partial \theta}\right)^2\right] \\
&\quad + \frac{1}{2r^2}\left(u_r^2 + u_\theta^2\right) + \frac{1}{r^2}\left[u_r \frac{\partial u_\theta}{\partial \theta} - u_\theta \frac{\partial u_r}{\partial r}\right] \\
2\varepsilon_{rz} &= \frac{\partial u_r}{\partial z} + \frac{\partial u_z}{\partial r} + \frac{\partial u_r}{\partial r}\frac{\partial u_r}{\partial z} + \frac{\partial u_z}{\partial r}\frac{\partial u_z}{\partial z} + \frac{\partial u_\theta}{\partial r}\frac{\partial u_\theta}{\partial z}
\end{aligned} \tag{10}$$

$$2\varepsilon_{r\theta} = \frac{1}{r}\frac{\partial u_r}{\partial \theta} + \frac{\partial u_\theta}{\partial r} - \frac{u_\theta}{r} + \frac{1}{r}\left[\frac{\partial u_r}{\partial r}\frac{\partial u_r}{\partial \theta} + \frac{\partial u_z}{\partial r}\frac{\partial u_z}{\partial \theta} + \frac{\partial u_\theta}{\partial r}\frac{\partial u_\theta}{\partial \theta}\right] + \frac{1}{r}\left[u_r\frac{\partial u_\theta}{\partial r} - u_\theta\frac{\partial u_r}{\partial r}\right]$$

$$2\varepsilon_{z\theta} = \frac{1}{r}\frac{\partial u_z}{\partial \theta} + \frac{\partial u_\theta}{\partial z} + \frac{1}{r}\left[\frac{\partial u_r}{\partial z}\frac{\partial u_r}{\partial \theta} + \frac{\partial u_z}{\partial z}\frac{\partial u_z}{\partial \theta} + \frac{\partial u_\theta}{\partial z}\frac{\partial u_\theta}{\partial \theta}\right] + \frac{1}{r}\left[u_r\frac{\partial u_z}{\partial z} - u_\theta\frac{\partial u_r}{\partial z}\right]$$

and

$$D = \frac{E(1-\nu)}{(1+\nu)(1-2\nu)} \cdot \left|\begin{matrix} 1 & \frac{\nu}{1-\nu} & \frac{\nu}{1-\nu} & 0 & 0 & 0 \\ & 1 & \frac{\nu}{1-\nu} & 0 & 0 & 0 \\ & & 1 & 0 & 0 & 0 \\ & & & \frac{1-2\nu}{2(1-\nu)} & 0 & 0 \\ & & & & \frac{1-2\nu}{2(1-\nu)} & 0 \\ \text{Symmetric} & & & & & \frac{1-2\nu}{2(1-\nu)} \end{matrix}\right|$$

Then if σ_0 is the initial stress vector one has :

$$\frac{\partial U}{\partial \delta} = \sum_{n=0}^{N} (K_{en} + K_{gn}(\sigma_0))\delta_n \qquad (11)$$

with

K_{en}, classical stiffness matrix
$K_{gn}(\sigma_0)$, geometric stiffness matrix, function of initial stresses.

Then from (6) and (11) and neglecting Coriolis effect, differential equations of the structure are obtained :

$$M_o\delta^{\circ\circ}_o + (K_{eo} + K_{go}(\sigma_0) - \Omega^2 M_{go})\delta_0 = F(\Omega^2) \qquad (12)$$

for n = 0, and

$$M_n.\delta^{\circ\circ}_n + (K_{en} + K_{gn}(\sigma_0) - \Omega^2 M_{gn})\delta_n = 0 \qquad (13)$$

for $n \neq 0$.

For the first step σ_0 is obtained from (12) by solving :

$$(K_{eo} + K_{go}(\sigma_0) - \Omega^2 M_{go})\delta_0 = F(\Omega^2) \qquad (14)$$

With an iterative Newton-Raphson procedure.

Next, for each n, frequencies and associated mode shapes are obtained from the matrix equations.

$$\omega^2 M_n \delta_n = (K_{en} + K_{gn}(\sigma_0) - \Omega^2 M_{gn})\delta_n \qquad (15)$$

by solving a classical eigenvalue problems using a simultaneous iterative technique.

The principles of calculation of the thin structures is the same and will not be presented here. Novozhilov thin shell theory has been used [6].

APPLICATION TO A REDUCTION GEAR

Experiments and calculations have been performed at rest ($\Omega = 0$). The mode shapes have been obtained from holographic measurements. The time average method has been used because it is much simpler than the real time or stroboscopic method and because the range of the frequencies to be measured (higher than 500 Hz) is very convenient.

The reduction gear is not exactly symmetric because of the 8 holes that can be observed in fig. 3 but we have neglected that effect. The finite element modelisation has been performed with this and thick elements.

. In figure 1 a cross-section of the reduction gear is presented

. In figure 2 finite element and experimental values for n between 0 and 8 are presented. The agreement is observed to be satisfactory.

. In figure 3 some photographs of time average holographic method are presented and mode shapes are observed to be very easy to definie using Fourier'series.

This explains the good agreement between theoretical and experimental results presented in figure 2.

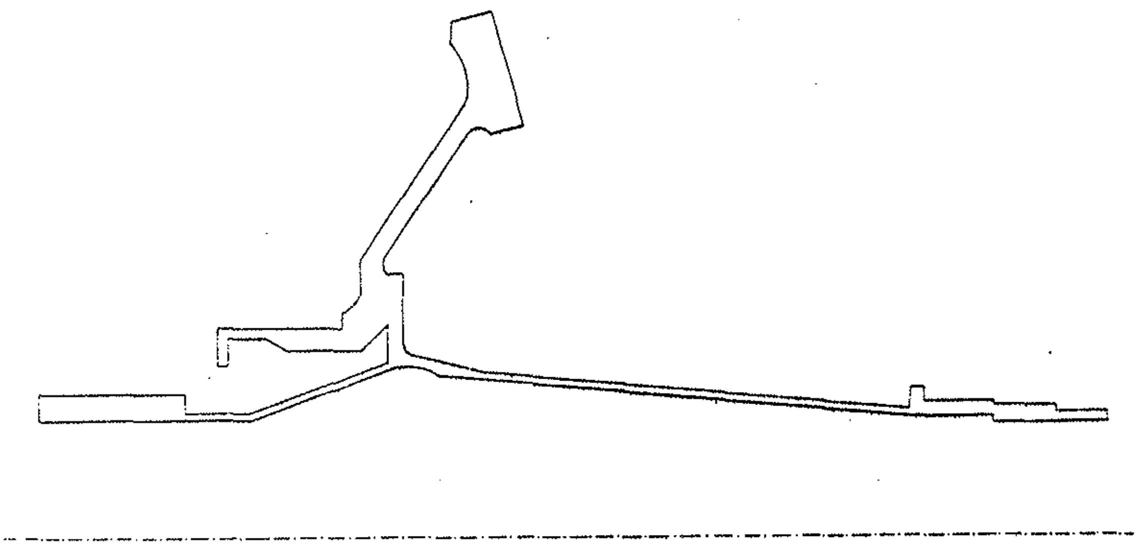

Figure 1: Cross-Section of the Reduction Gear

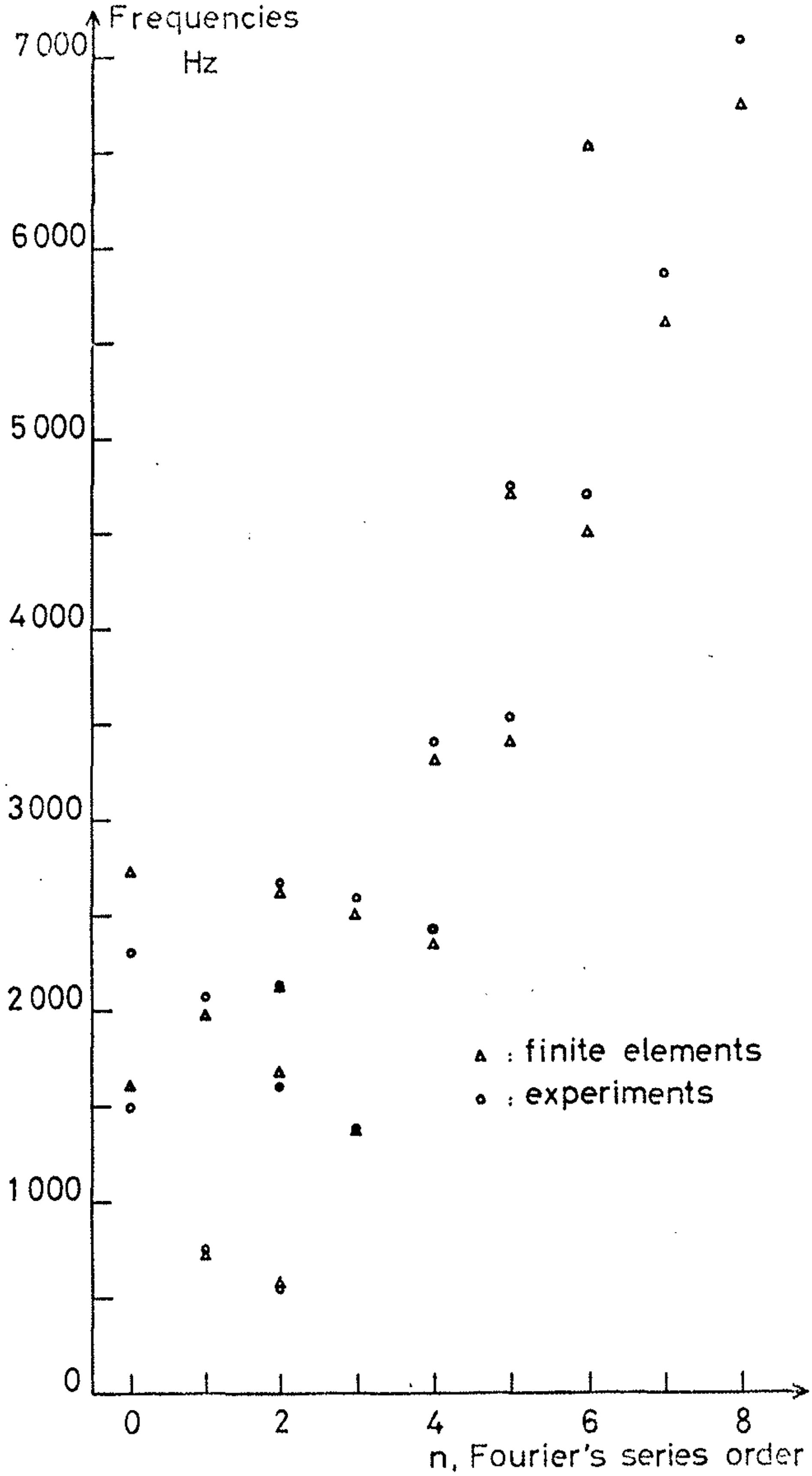
Frequencies
Hz
7 000
6 000
5 000
4 000
3000
2 000
1 000
0
0
2
4
6
8
n, Fourier's series order
▲ : finite elements
∘ : experiments

figure 2

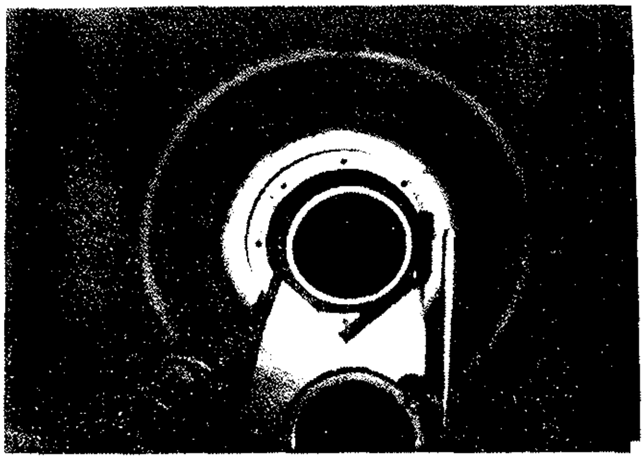

n=0

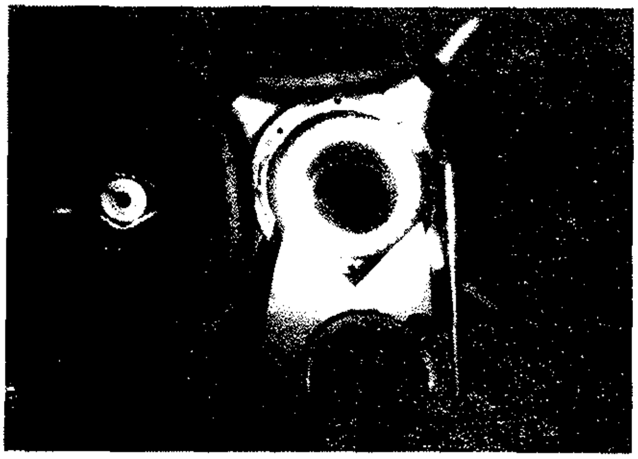

n=2

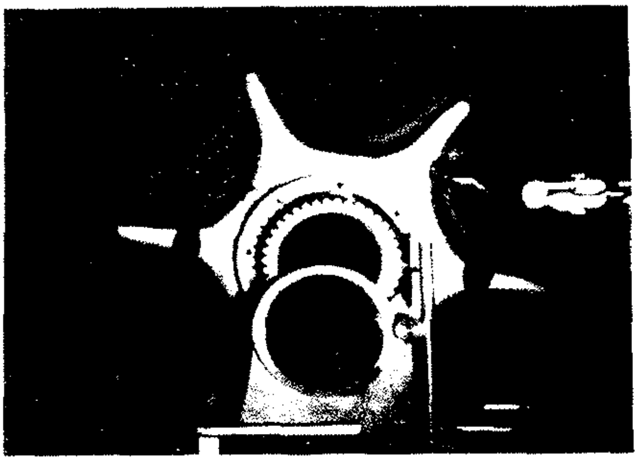

n=3

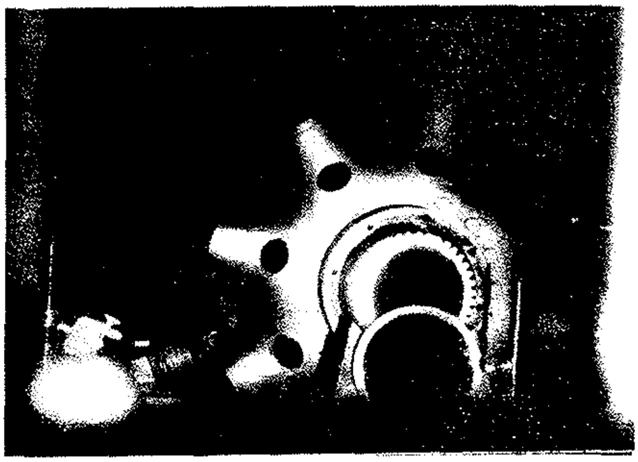

n=4

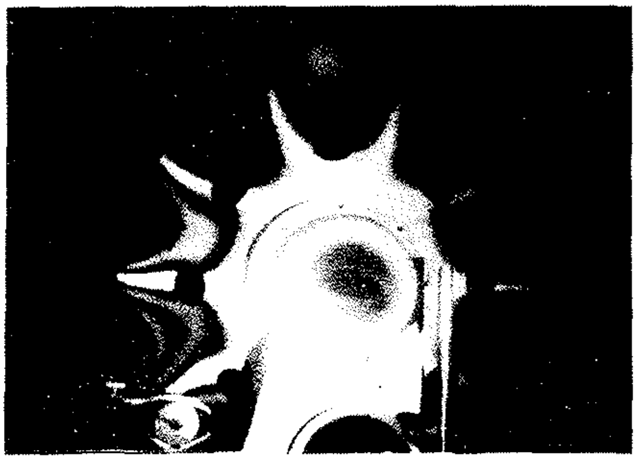

n=5

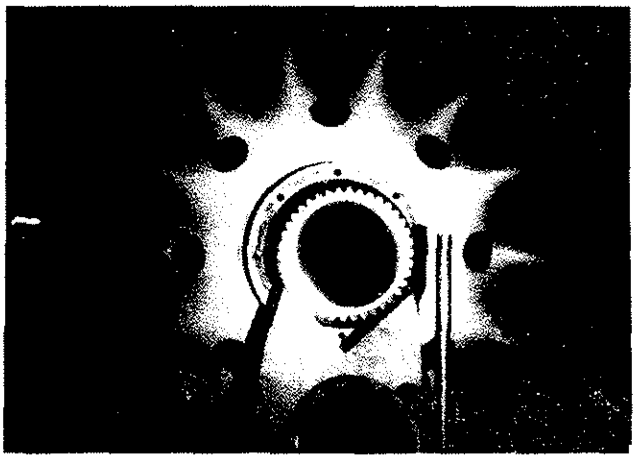

n=7

Figure 3 : Mode shapes for different Fourier's series orders

EXTENSION OF THIS WORK

A conclusion of these results is that the finite element model obtained is convenient and that is can be used easily to predict the change in the behaviour of the structure when a slight modification in the structure is performed.

The procedure may be the following. For n if ω_i, δ_{ni}, is a solution one has :

$$\omega_i^2 \cdot \delta_{ni}^t \cdot M_n \cdot \delta_{ni} = \delta_{ni}^t \cdot K_n \cdot \delta_{ni} \tag{16}$$

and $\delta_{ni}^t\ M_n\ \delta_{ni}$ and $\delta_{ni}^t\ K_n\ \delta_{ni}$ have been obtained in solving (15).

If M_n and K_n became respectively $M_n + \Delta M_n$, $K_n + \Delta K_n$ the frequency ω_i will be changed in $\omega_i(\Delta)$ and obtained from Rayleigh method :

$$\omega_i^2(\Delta) \cdot \delta_{ni}^t (M_n + \Delta M_n) \delta_{ni} = \delta_{ni}^t (K_n + \Delta K_n) \delta_{ni} \tag{17}$$

Then only calculation, needed are those of $\delta_{ni}^t \cdot \Delta M_n \cdot \delta_{ni}$ and $\delta_{ni}^t \cdot \Delta K_n \cdot \delta_{ni}$ which are fairly straight forward.

AKNOWLEDGMENTS

This work was supported by the Société Nationale Industrielle Aérospatiale and The Direction des Recherches et Moyens d'Essais. The authors are indebted to S.N.I.A.S. and D.R.M.E. for permission to publisch this paper.

REFERENCES

[1] D. Bushnell, Analysis of ring stiffened shells of revolution under combined thermal and mechanical loading.
A.I.A.A. Journal, vol. 9, n° 3, 1971.

[2] D. Bushnell, Stress stability and vibration of complex branched shells of revolution.
Analysis and user's manual of Bosor IV.

[3] S. Ghosh, E. Wilson, Dynamic stress analysis of axisymmetric structure under arbitrary loading.
Report E.E.N.C. 69-10, sept. 1969.

[4] P. Trompette, M. Lalanne, Frequencies and mode shapes of geometrically axisymetric structures : application to a jet engine.
46th Shock and Vibration Bulletin, 1976.

[5] P. Trompette, Etude dynamique des structures - Effet de rotation, amortissement.
Thèse de Doctorat d'Etat, 1976.

[6] V. Novozhilov, Thin shell theory.
Wolters-Noordhoff, 1970.